nature portfolio

https://doi.org/10.1038/s41596-023-00805-y

Supplementary information

A flow cytometry-based protocol for syngenic isolation of neurovascular unit cells from mouse and human tissues

In the format provided by the authors and unedited

Supplementary Figure 1

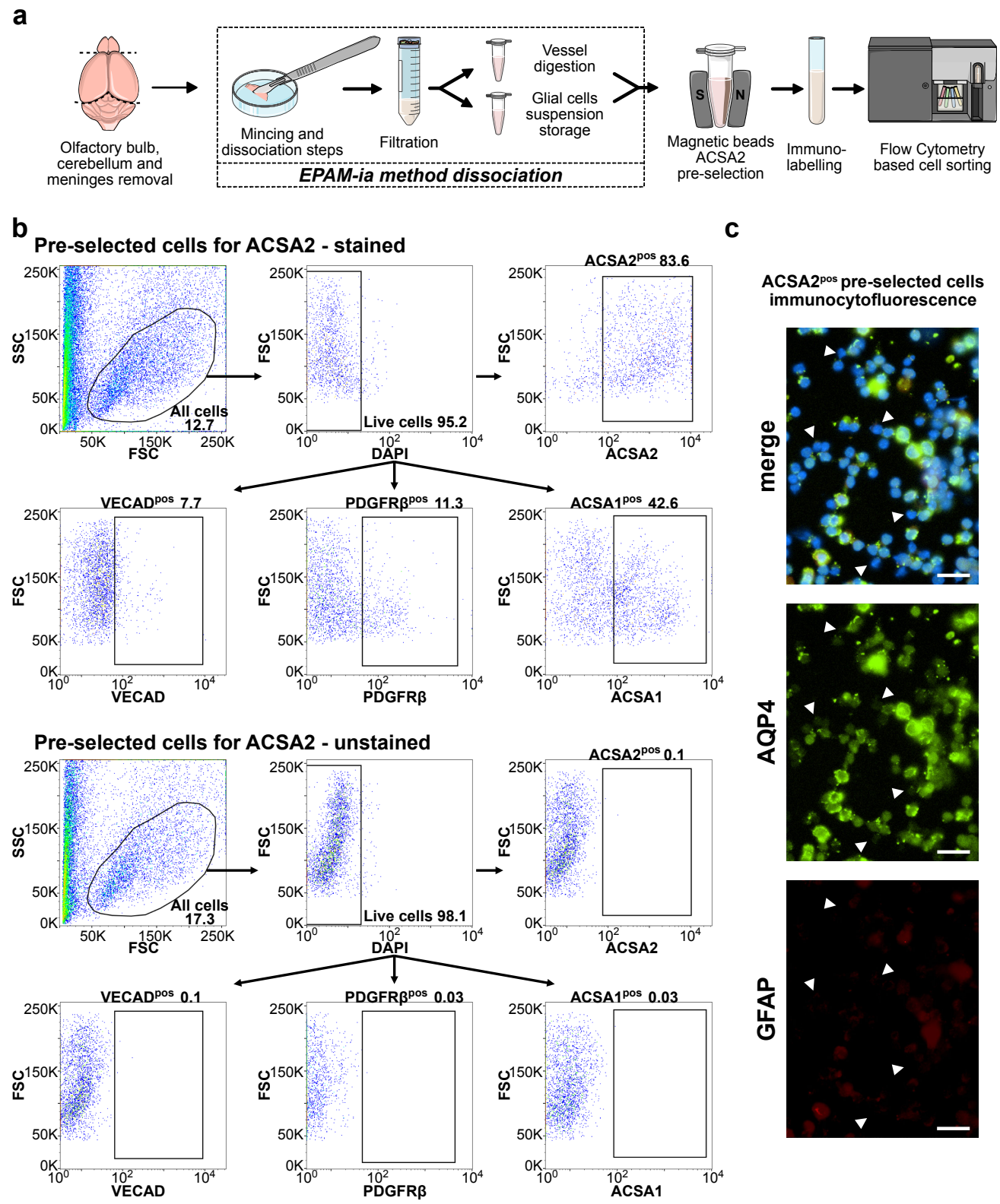

Figure S1. Purity of cells isolated by magnetic beads

(a) Brain cell suspension obtained by EPAM-ia method using the kit-based digestion mix 1 was subjected to pre-selection for ACSA2 using magnetic beads, followed by immunolabeling and flow cytometry. **(b)** Majority of live cells preselected using ACSA2 magnetic beads are positive for ACSA2 by FACS, however a significant percentage did not stain for ACSA2 indicating presence of other cells clumped to ASCA2^{pos} cells collected with the magnetic beads. There were numerous cells that were positive for VE-cadherin and PDGFRβ, indicating contamination with endothelial cells and mural cells respectively of ACSA2^{pos} astrocytes isolated using magnetic beads. ACSA1 (GLAST) another marker for astrocytes stained only part of the cell population selected with ASCA2, suggesting ASCA2 as a better marker of astrocytes compared to ACSA1. Percentages refer to the proportion of cells in the previous parent gate. First SSC/FSC plot shows 500,000 events for the stained and unstained samples. **(c)** A fraction of the ACSA2^{pos} cells collected with the magnetic beads was further stained by immunofluorescence. As pointed by the arrowheads, some viable cells do not express astrocytic markers suggesting a contamination by other cell types when using the magnetic beads. Scale = 20µm. Panel **a** adapted with permission from ref.31, Springer.

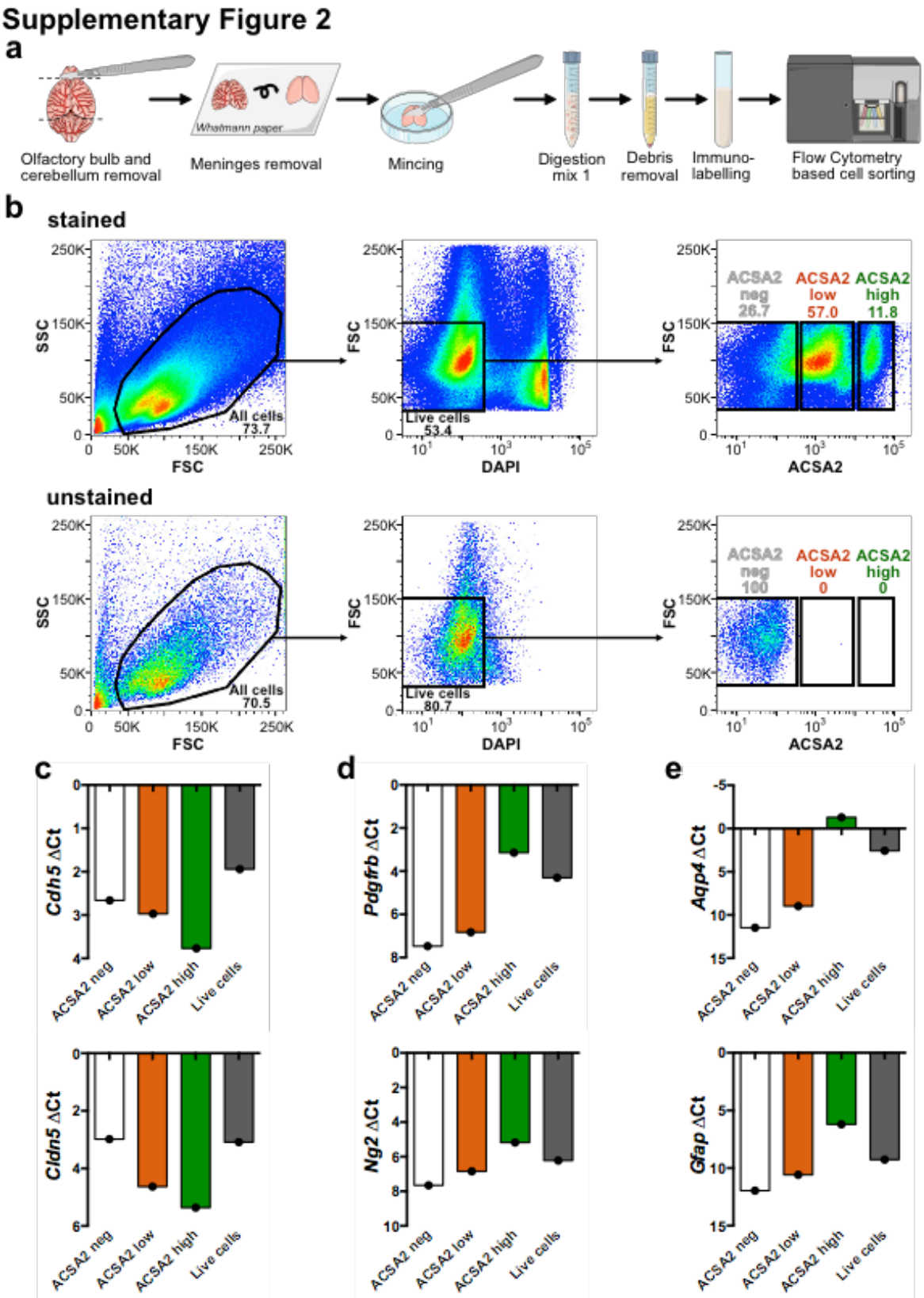

Figure S2. Determination and isolation of the astrocyte population as ACSA2^{high} stained cells.
(a) After cerebrum is separated from olfactory bulb, brain stem and cerebellum, the meninges and large extraparenchymal blood vessels are removed by rolling the tissue on sterile Whatmann paper. Minced tissue is then digested with a commercially available enzyme mix before myelin and debris are eliminated with the debris removal solution form the same kit. The pellet is resuspended and incubated with fluorescently conjugated ACSA2 antibody for flow cytometry based cell sorting. **(b)** After excluding the debris (left panel), live cells are selected (DAPI^{neg}, middle panel) and gated for ACSA2 (right panel). To identify the population containing the astrocytes, the ACSA2^{neg}, ACSA2^{low}, ACSA2^{high} (right panel) as well as live cell populations (middle panel) are collected. Percentages refer to the previous parent gate. First SSC/FSC plot shows 1,000,000 and 100,000 events for the stained and unstained samples, respectively. FSC, forward-scatter area; SSC, side-scatter area. **(c-e)** Quantitative PCR (qPCR, n=1 using 3 mice) purity control results on ACSA2^{neg}, ACSA2^{low}, ACSA2^{high} and live cell populations assessing expression levels of markers for endothelial cell with *Cdh5* and *Cldn5* **(c)**, pericyte with *Pdgfrb* and *Ng2* **(d)** and astrocyte with *Aqp4* and *Gfap* **(e)**. If no amplification was detected, the ΔCt value is set at 15 by default. Panel **a** adapted with permission from ref. 31, Springer.

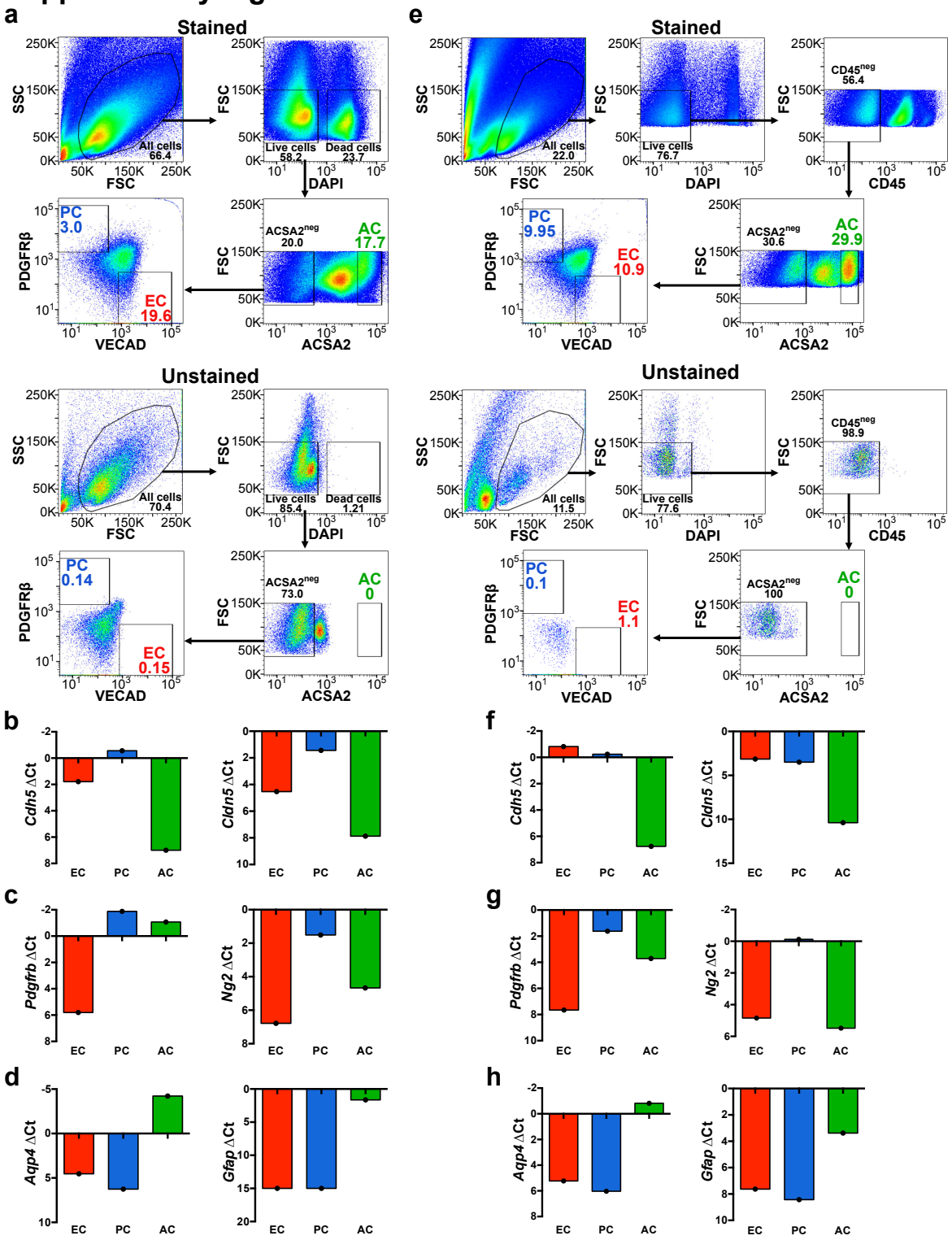

Figure S3. Isolation and purity enrichment of astrocytes, endothelial cells and pericytes with anti-CD45 antibody. **(a)** Initial gating strategy starting with exclusion of debris (stained panel, top left) and selection of live cells (stained, top right) further plotted for ACSA2. Astrocytes (AC) are collected as ACSA2^{pos} cells (stained, bottom right). ACSA2^{neg} cells are plotted for isolation of endothelial cells (EC) defined as ACSA2^{neg}/VE-cadherin^{pos}/PDGFRβ^{neg} cells (stained, bottom left). On the same plot, pericytes (PC, mural cells) are also sorted as ACSA2^{neg}/VE-cadherin^{neg}/PDGFRβ^{pos} cells. The same gating strategy is applied to the unstained control. Percentages refer to the proportion of cells in the previous parental gate. First dot plots show 1,000,000 and 100,000 events for the stained and unstained samples, respectively. FSC, forward-scatter area; SSC, side-scatter area. **(b-d)** Purity of sorted cells is assessed by qPCR targeting markers for endothelial cells (**b**, *Cdh5*, *Cldn5*), pericytes (**c**, *Pdgfrb*, *Ng2*) and astrocytes (**d**, *Aqp4*, *Gfap*). **(e)** In order to eliminate the blood immune cells, CD45 staining is added in the gating strategy as following. Debris (top left) and dead cells (DAPI^{pos} cells, top middle) are excluded. Live cells (top middle) are plotted for CD45 (top right panel). Astrocytes, endothelial cells and pericytes populations are determined as already described in part (a) from the CD45^{neg} cell population (stained, bottom panels). The same gating strategy is employed for the unstained control. **(f-h)** Purity of sorted cells is assessed by qPCR targeting markers of endothelial cells (**f**, *Cdh5*, *Cldn5*), pericytes (**g**, *Pdgfrb*, *Ng2*) and astrocytes (**h**, *Aqp4*, *Gfap*). If no amplification was detected, the ΔCt value is set at 15 by default.

Supplementary Figure 4

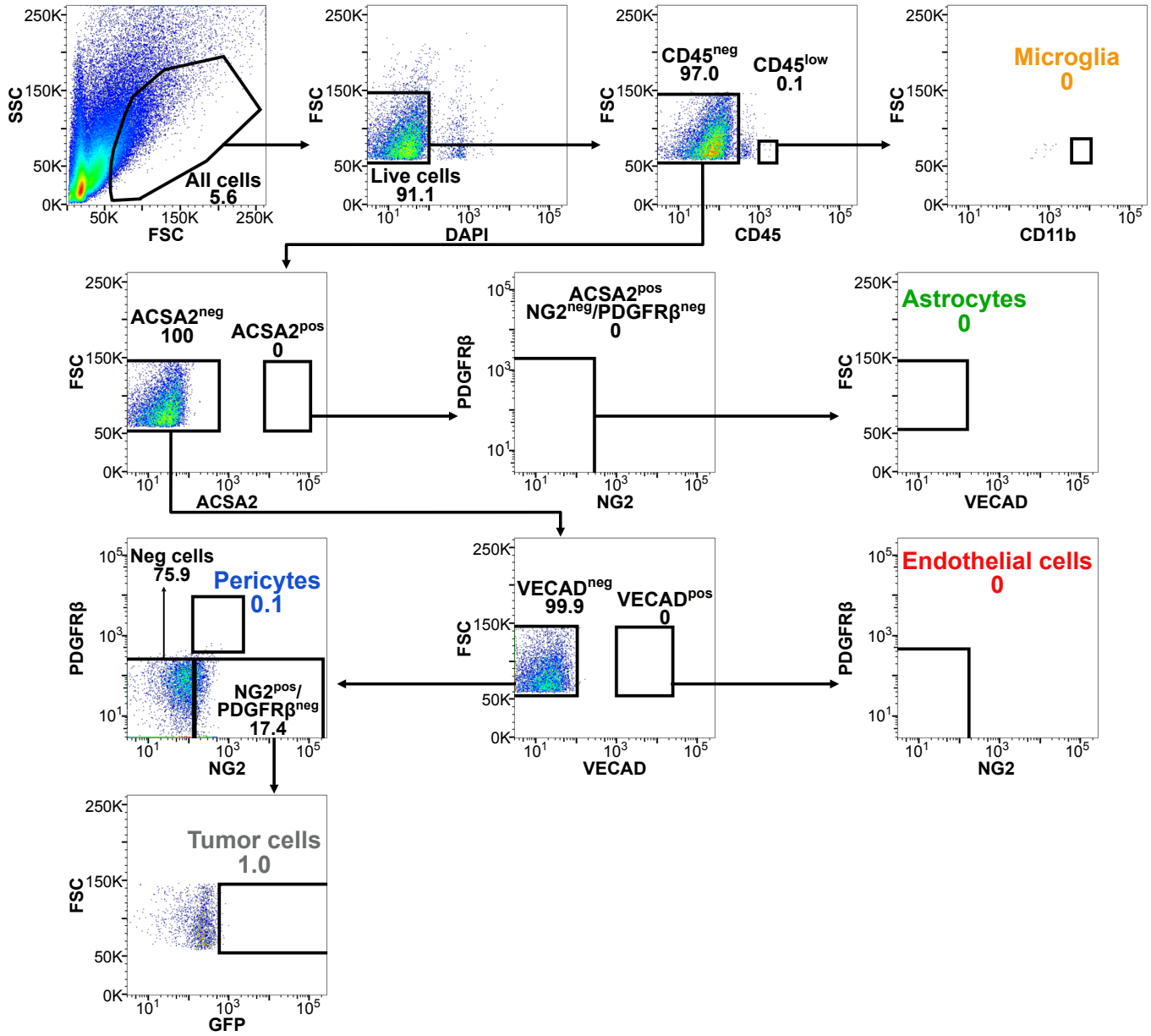

Figure S4. Unstained control of neurovascular unit and tumor cells isolated using EPAM-ia method applied to a murine model of brain metastasis.

FACS dot plots showing unstained control for the selected surface antigens and the FITC channel used for NVU and tumor cells isolation in the mouse melanoma metastasis model. Percentages refer to the proportion of cells in the previous parent gate. First FSC/SSC plots shows 100,000 events. FSC, forward-scatter area; SSC, side-scatter area.

Supplementary Figure 5

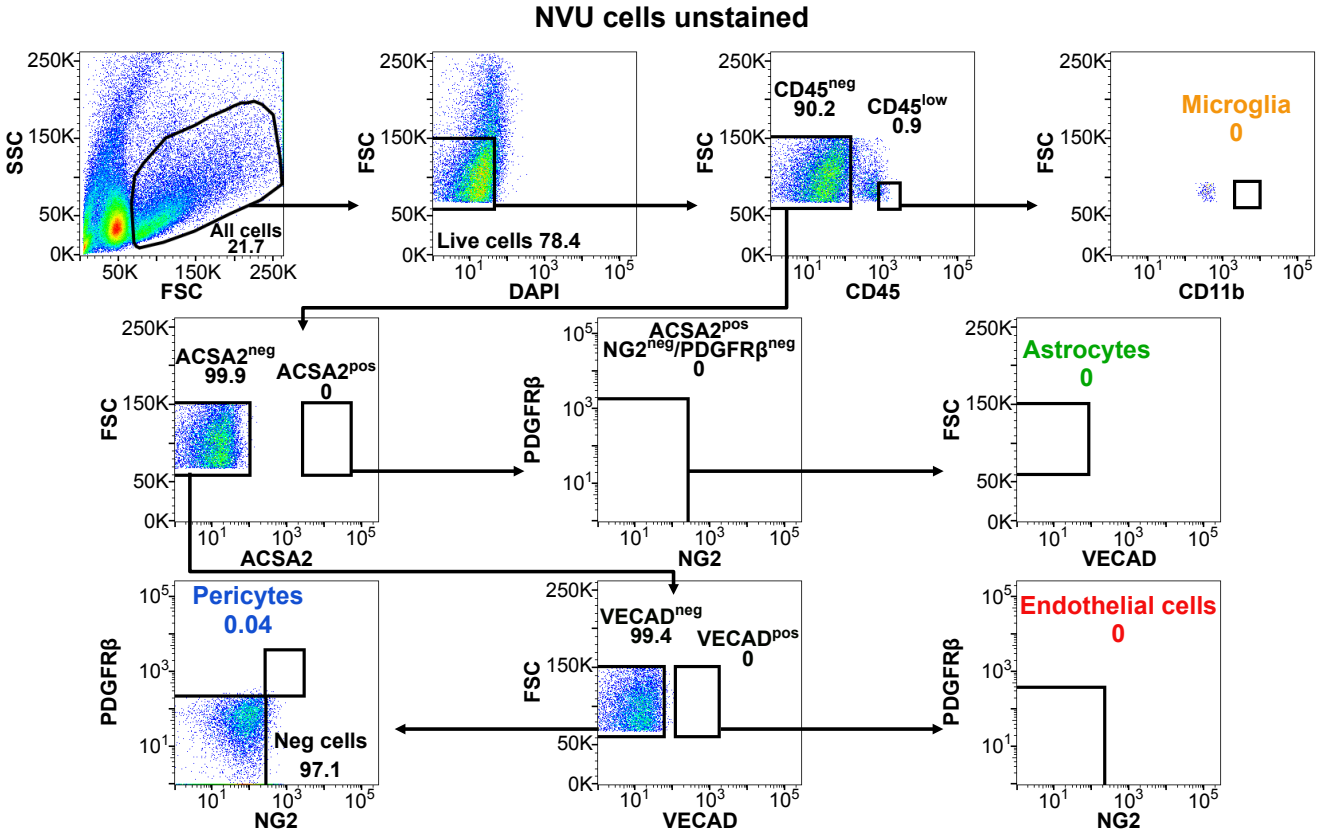

Figure S5. Unstained control of neurovascular unit and tumor cells isolated using EPAM-ia method applied to a murine model of glioblastoma.

FACS dot plots showing unstained control for the selected surface antigens used for NVU cells isolation in the mouse glioblastoma model. Percentages refer to the proportion of cells in the previous parent gate. First FSC/SSC plots shows 100,000 events. FSC, forward-scatter area; SSC, side-scatter area.

Supplementary Figure 6

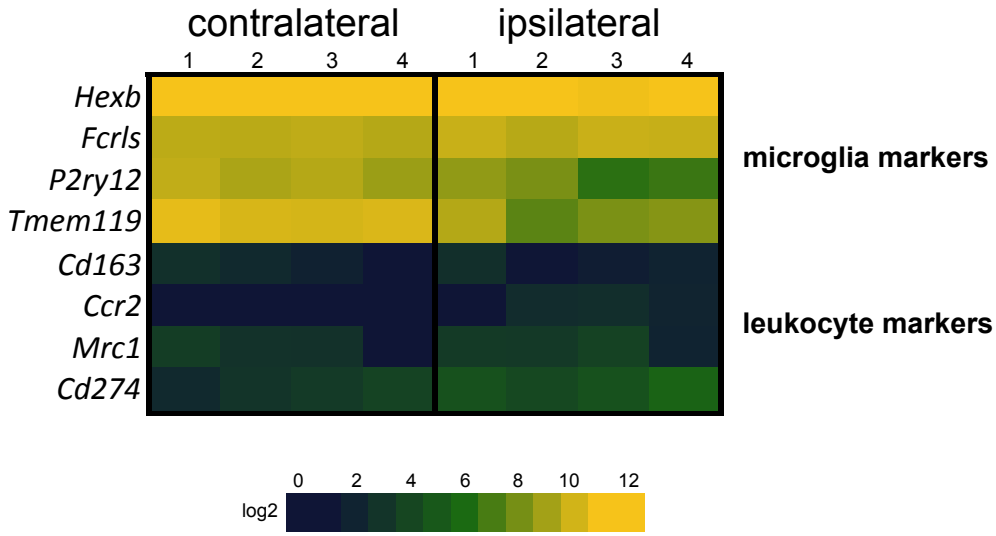

Figure S6. Enrichment analysis of the isolated microglia population in stroke.
Heatmap representing log2 expression of selected microglial and leukocyte cell-specific marker genes in the microglia population isolated from ischemic and contralateral mouse cerebrum applying the EPAM-ia method (n=4). This heatmap shows that the isolated microglia ($CD45^{low}/CD11b^{pos}$) are rather pure, as they express leukocyte markers to a very low level, which is comparable between the healthy contralateral and ischemic ipsilateral hemispheres.

Supplementary Figure 7

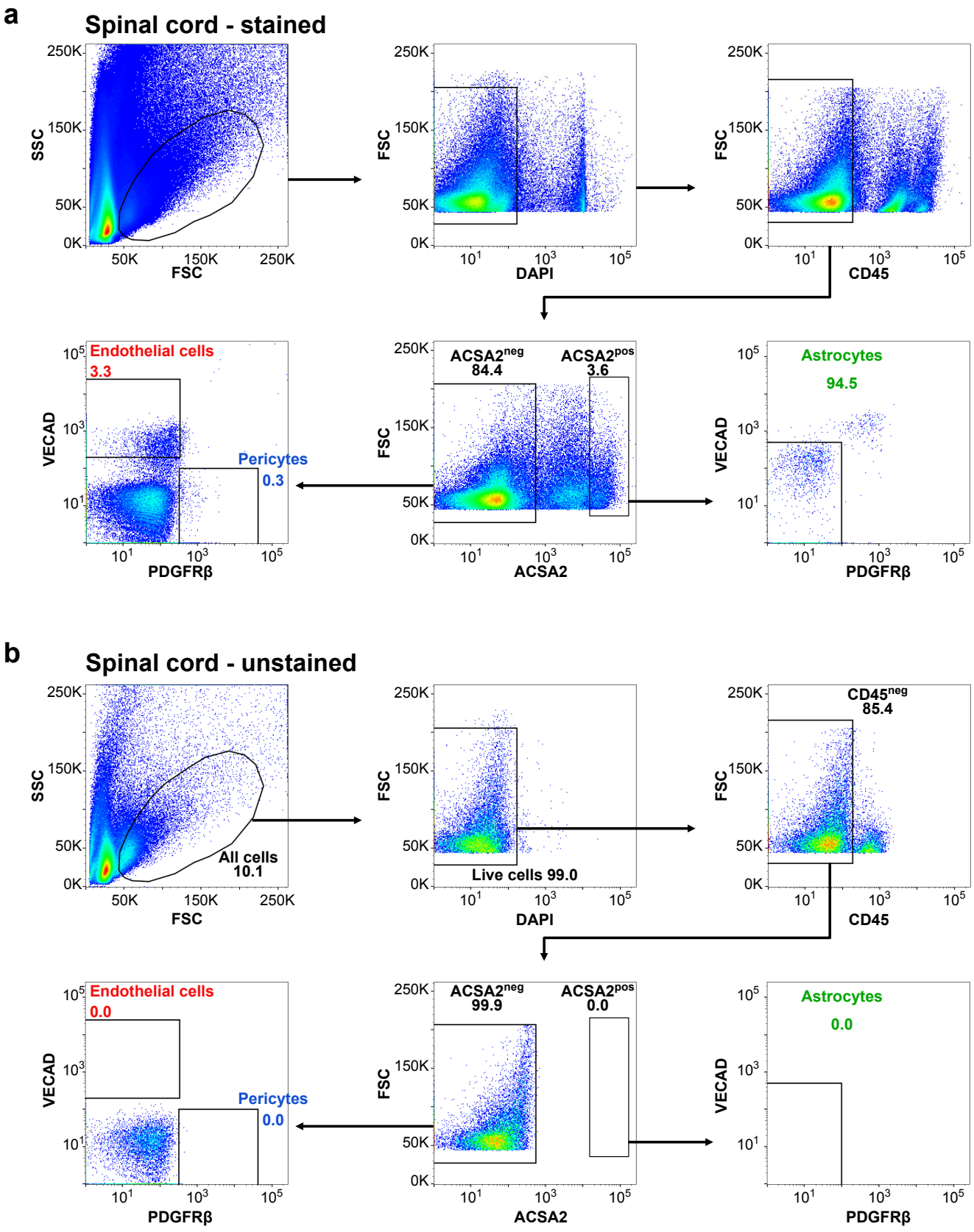

Figure S7. Isolation of NVU cells from spinal cord using EPAM-ia method
(a) Gating strategy for the isolation of NVU cell-types from mouse spinal cord tissue digested according to the EPAM-ia protocol. **(b)** Unstained control spinal cord sample showing specificity of staining post isolation of cells with EPAM-ia protocol. The FACS plots are representative of two independent spinal cord samples subjected to EPAM-ia based isolation. Percentages refer to the proportion of cells in the previous parent gate. First FSC/SSC plot shows 4,000,000 events and 500,000 events in the stained and unstained samples, respectively.

Supplementary Figure 8

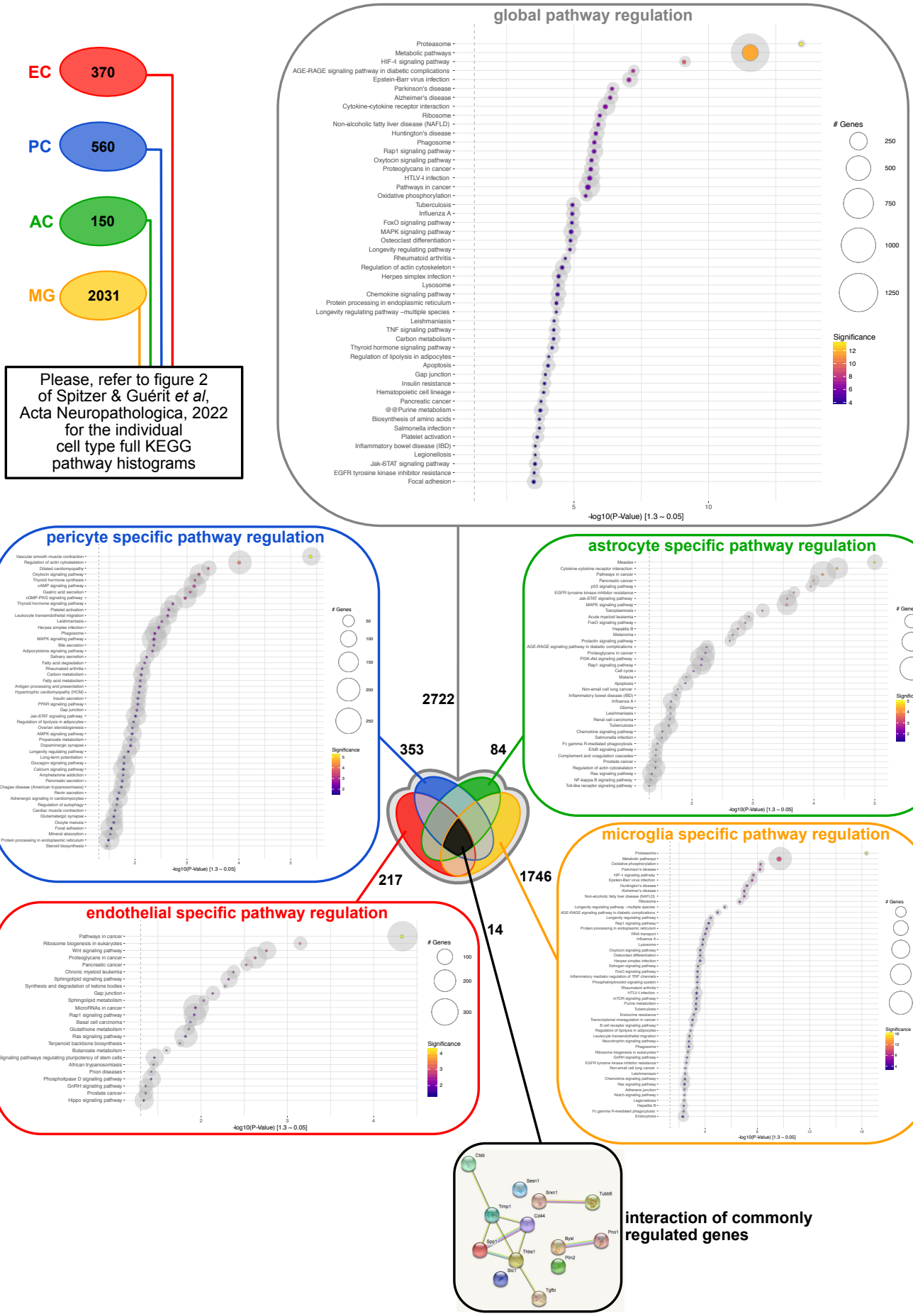

Figure S8. KEGG histograms revealing the most relevant activated pathways after stroke induction. Pathway regulation was assessed considering the complete dataset combining the regulated genes from all the NVU cell types (top histogram). Regulated genes were also analyzed to reveal significantly regulated KEGG pathways in the NVU cell types in a cell specific manner (middle histograms). The regulated genes common to all 4 cell types (bottom illustration) were analyzed with string-db.org database as the KOBAS analysis could not be performed with few genes (n=6, 3-4 mice/preparation).